J Solid State Electrochem (2004) 8: 748–756
DOI 10.1007/s10008-004-0541-x

ORIGINAL PAPER

Renata Solarska · Bruce D. Alexander
Jan Augustynski

Electrochromic and structural characteristics of mesoporous WO_3 films prepared by a sol-gel method

Received: 18 March 2004 / Accepted: 10 April 2004 / Published online: 3 July 2004

Abstract The preparation of electrochromic films of mesoporous tungsten trioxide from tungstic acid and tungstic hexaethoxide precursors with the addition of an organic stabiliser via a sol-gel method is reported. These films have been structurally characterised and both the film morphology and crystalline composition of the films were found to be significantly dependent on the temperature at which the films were annealed and upon the choice of precursor. Films annealed at lower temperatures consisted of amorphous and hexagonal tungsten trioxide, whereas films annealed above 500 °C comprised solely of monoclinic WO_3. The electrochromic activity of the films was found to be equally dependent on method of preparation, and both the composition and the structure of the WO_3 films were shown to clearly influence the colouration efficiency of the films.

Keywords Tungsten trioxide · Mesoporous film · Electrochromism · Raman spectroscopy · Sol-gel synthesis

Introduction

The tailoring of microporous and mesoporous oxide films has recently attracted the attention of chemists in view of numerous potential applications associated with it, including heterogeneous catalysis, chemical separation, optoelectronics, sensors, batteries, and photonic and electrocatalytic materials. Although most of the effort has initially been devoted to the formation of mesoporous, amorphous silica oxides [1, 2, 3], the interest then extended to metallic oxides with charge transport and transfer functionalities [4, 5, 6].

Among a variety of available film deposition techniques, the sol-gel method provides great potential for controlling film morphology and, particularly, porosity. In some cases the sol-gel processing may involve acidification of a basic metal salt, followed by condensation of the formed acid, evaporation of the solvent, and finally annealing at relatively high temperature. Metal alkoxides are frequently used alternative precursor species, and after hydrolysis these undergo condensation to form a sol. Both the choice of the precursor composition and the manipulation of the processing conditions (particularly the annealing temperature) allow us to tailor the porosity and particle size of sol-gel derived oxides. For example, the change of the processing conditions from acidic to basic will normally favour formation of mesoporous (pore diameters between 2 and 50 nm) instead of microporous (pore diameters less than 2 nm) films.

On the other hand, structural ordering of the oxide films that occurs during heat treatment is normally achieved by the addition of a structure-directing species to the sol or to the gel. However, in many cases the template-mediated, ordered mesostructures tend to collapse during the high-temperature heat treatments required to form well-crystallized films. The extent of crystallinity determines the magnetic and electronic properties of the films and, importantly, their electrical conductivity, which is strongly affected by the nature of the grain boundaries [7].

We recently described the synthesis of such well-crystallized mesoporous WO_3 films that can be obtained using a tungstic acid precursor and low molecular weight poly(ethylene glycol) 200 or 300, which plays the role of both a stabilizing and a structure-directing agent [8]. Formation of a complex between tungstic acid and the hydrophilic poly(ethylene glycol) species, inferred from the thermogravimetric and differential thermal analysis data, distinctly affects the crystallization process of WO_3, leading first (at ~200 °C) to the formation of metastable hexagonal tungsten trioxide. It is only above

Dedicated to Zbigniew Galus on the occasion of his 70th birthday.

R. Solarska · B. D. Alexander · J. Augustynski (✉)
Département de Chimie Minérale, Analytique et Appliquée,
Université de Genève, quai E.-Ansermet 30,
1211 Genève, Suisse
E-mail: jan.augustynski@chiam.unige.ch
Fax: +41-22-3796830

400 °C that the conversion into a stable monoclinic form of WO_3 starts, accompanied by the combustion of the remaining organic matter. The resulting mesoporous WO_3 films consist of plate-like nanocrystals with typical sizes of ~10–30 nm and with slightly larger mesopores. Annealing the films at temperatures above 500 °C causes their rapid sintering, reflected by the increase in particle and pore sizes. A distinct morphological feature of these films is the preferential orientation of the 200, 020 and 002 faces of WO_3 crystallites parallel to the conducting glass substrate, which is preserved even after heating at high temperatures. This may explain the good transparency of such mesoporous WO_3 films to a large portion of the visible spectrum.

The primary reason for our interest in nanostructured WO_3 films was the development of efficient photoanodes for water splitting under visible light illumination. In fact, films of a thickness of a few microns, obtained using the tungstic acid/PEG precursor, exhibit particularly promising photoelectrochemical properties. Their photoresponse extends into the blue region of the solar spectrum, up to 500 nm, with the photocurrent densities for the photoelectrolysis of water, recorded in acidic solutions under AM 1.5 irradiation, reaching 4 mA/cm^2 [9]. Due to their nanocrystalline nature resulting in an open and porous structure, and their smoothness (maximum protuberance being less than 20 nm), these films also appear to be potentially interesting electrochromic materials. In fact, they combine excellent transparency to wavelengths larger than 550 nm with a short diffusion path for intercalating cations (Li^+, H^+). Here, changes in optical properties and the degree of electrochromic optical modulation are presented for the WO_3 films obtained using both tungstic acid and tungsten hexaethoxide precursors annealed over a range of temperatures. Structural modifications of WO_3 observed using Raman microscopy are related to the electrochromic colouration efficiencies of the films.

Materials and methods

Preparation

Fresh tungstic acid was prepared by elution of an aqueous solution of Na_2WO_4 through a proton exchange resin (Dowex 50 WX2–200, 100–200 mesh). In order to retard the condensation of tungstic acid, and therefore the formation of polyoxoanions, the eluted solution was collected in ethanol under continuous stirring. Upon completion of the elution, the solution was reduced in vacuo to a concentration of ~0.5 M before addition of poly(ethylene glycol) 300 (PEG) such that the PEG/WO_3 ratio was of the order of 0.5 w/w.

Films were also prepared from a tungsten (VI) ethoxide precursor. PEG 300 was added to anhydrous tungsten (VI) ethoxide, 5% w/w ethanol (Alfa Aesar) before being applied to the conducting glass substrates. The substrates were then dried and heated as described above.

The WO_3 films were prepared by spreading a small quantity of the precursor solution onto a conducting glass substrate, consisting of a 0.5 μm F-doped SnO_2 overlayer (Nihon Sheet Glass Co., 12 Ω/sq.). Films were dried at room temperature for 10 min before annealing in flowing oxygen for 30 min in the range 250–550 °C.

Characterisation

The crystalline composition of the samples has been analysed by Raman microscopy. Raman spectra were recorded using a LabRam I Raman confocal microscope, fitted with an air-cooled CCD camera. Excitation at 532.0 nm was provided by a frequency doubled Nd:YAG laser; the laser power at the sample was 25–110 μW, depending on the sample, minimising photodegradation or photobleaching of the sample. Use of a 100× objective (Olympus, N.A. 0.90) and a pinhole of 300 μm ensured an estimated sampling depth of 3 μm. The spectrometer was calibrated against Ne emission and the 520 cm^{-1} Raman signal of a Si wafer. Spectral resolution was typically 2 cm. Spectra were recorded from a number of positions on the surface and were found to be highly reproducible.

UV-Vis transmission spectra were recorded on a Perkin Elmer, Lambda 900 spectrophotometer. The morphology of the samples was examined using a LEO Gemini 982 scanning electron microscope (SEM) equipped with a Röntec energy dispersive X-ray analysis (EDX) detector system.

Electrochromic measurements were performed in either a 1 M $LiClO_4$ solution in propylene carbonate or 1 M aqueous H_2SO_4 solution using electrodes consisting of 0.4 μm thick WO_3 films. The photoelectrochemical activity was tested in a 1 M $H_2SO_{4(aq)}$ solution by illuminating the WO_3 electrode from the side of the electrolyte:film interface in a Teflon cell equipped with a quartz window. The counter and reference electrodes were a large area Pt foil and a saturated calomel electrode, respectively. The WO_3 electrodes were illuminated with simulated solar AM 1.5 light, obtained using a 150 W xenon lamp fitted with a Schott 113 filter and neutral density filters. The wavelength photoresponse (the quantum efficiency of the photocurrent versus excitation wavelength) of the WO_3 electrodes was determined using a 500 W xenon lamp (Ushio UXL-502HSO) set in an Oriel model 66021 housing and a Multispec 257 monochromator (Oriel) with a typical bandwidth of 4 nm. The intensity of the incident light from the monochromator was measured using a model 730 A radiometer/photometer (Optronic Lab).

All solutions were prepared with analytical grade reagents and were thoroughly degassed with nitrogen prior to measurement. Aqueous solutions were prepared with Milli-Q water. Photoelectrochemical and electrochromic measurements were carried out under

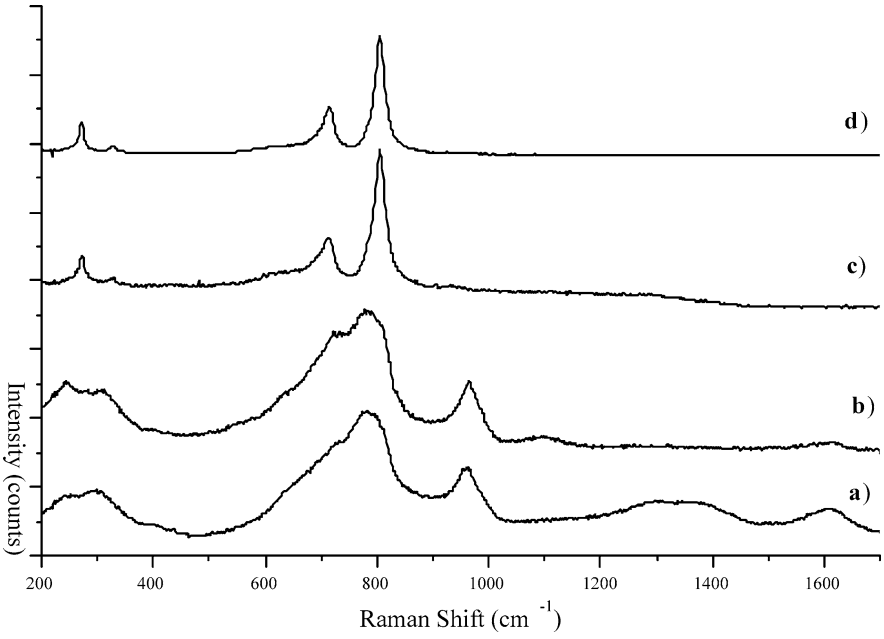

Fig. 1 Raman spectra of WO_3 films derived from a tungstic acid precursor deposited on conducting glass substrates. Films annealed at **a** 350 °C; **b** 400 °C; **c** 500 °C; **d** 550 °C. The spectra shown in **a** and **b** were recorded using a laser power at the sample of 110 μW, whereas the spectra in **c** and **d** were recorded at 24 μW. The spectra of the films annealed at 400 °C and 500 °C have been multiplied by a factor of 2

potential-controlled conditions using an EG&G Princeton Applied Research Model 362 potentiostat.

Results and discussion

Raman spectra

Thin films of WO_3 have been prepared by annealing over a range of temperatures. Raman microscopy has been used to elucidate the crystalline composition of these films. The Raman spectra of the WO_3 films prepared from tungstic acid are shown in Fig. 1. Films were also prepared after annealing at lower temperatures but these films displayed poor adhesion to the conducting glass substrate and so will not be discussed herein. The spectrum of the WO_3 films produced after annealing at 350 °C (Fig. 1a) shows two strong bands at 780 and 962 cm^{-1} along with medium intensity bands centred around 1336 and 1610 cm^{-1}. Shoulders also appear at 635 and 732 cm^{-1}. These bands do not correspond to any known crystalline forms of WO_3 or hydrated oxides.

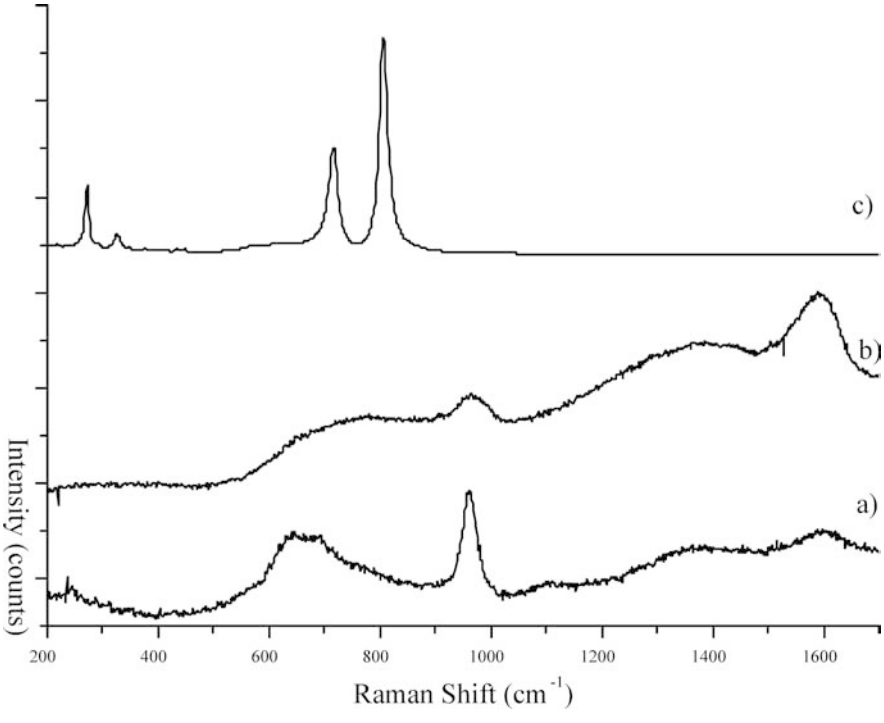

Fig. 2 Raman spectra of deposited WO_3 films that were derived from a tungsten (VI) ethoxide precursor deposited on conducting glass substrates. Films were annealed at **a** 500 °C; **b** 300 °C; **c** 300 °C followed by additional annealing at 550 °C

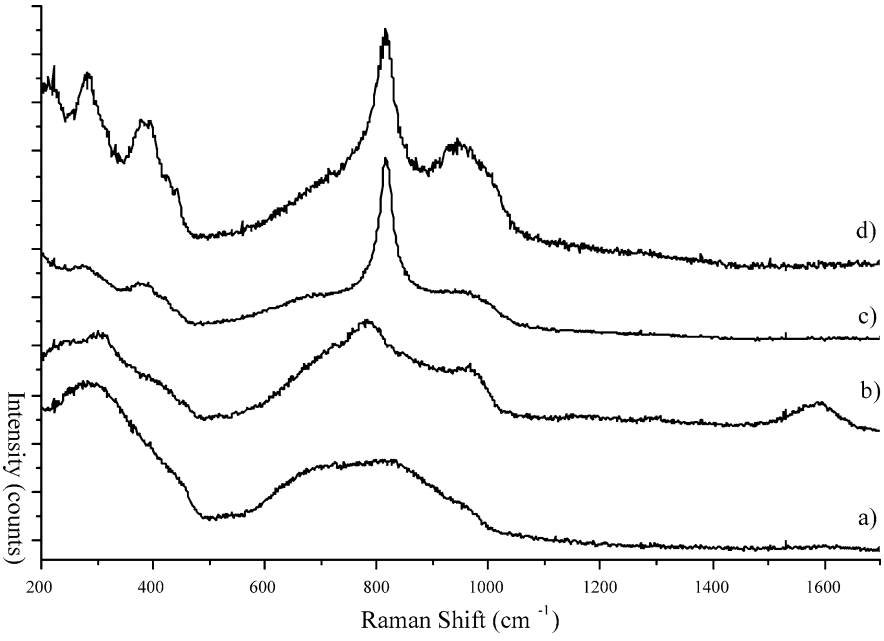

Fig. 3 Raman spectra of WO_3 films derived from a tungstic acid precursor deposited on conducting glass substrates after insertion of H^+ ions. Films were annealed at **a** 350 °C; **b** 400 °C; **c** 500 °C; **d** 550 °C. For the spectra presented in **c** and **d**, the laser power should not exceed 24 μW due to the rapid photobleaching that occurs at high incident laser powers

Nevertheless, the band present at 962 cm^{-1} is typical of the stretching mode of terminal W = O groups in tungsten oxide hydrates [10, 11]. The bands at 780 cm^{-1} and the shoulder at 732 cm^{-1} are ascribed to stretching modes involving O–W–O bridging oxygens, although the exact form of the species responsible remains unclear. Nevertheless, the form of the spectrum from 200–1700 cm^{-1} closely resembles that of amorphous WO_3 although the presence of the hexagonal phase of WO_3 cannot be discounted [12]. Following the work of Daniel et al, the weak band at 242 cm^{-1} and the shoulder at 635 cm^{-1} may be ascribed to h–WO_3, and it is entirely possible that the remaining h–WO_3 band at 817 cm^{-1} may be hidden by the broad hydrate band [11]. There are two important additional bands at 1336 and 1610 cm^{-1} present in the spectrum of the film annealed at 350 °C that cannot be attributed to a form of tungsten oxide. These bands are assigned to disordered graphitic carbon and are commonly present due to the incomplete combustion of organic matter (PEG). It should be stressed that apart from these two bands, no evidence for PEG has been found.

Few changes in band positions occur after annealing the WO_3 films at 400 °C. The most noticeable difference between Figs. 1a and b is that the carbon content is reduced by annealing at the higher temperature, indicating the near complete combustion of PEG. Bands previously ascribed to the presence of an unidentified hydrated amorphous phase are lowered in intensity to the point that the bands at 244 and 641 cm^{-1} due to hexagonal WO_3 become resolved. A band at 723 cm^{-1} is now clearly present, and this is ascribed to the start of the formation of the monoclinic WO_3 phase. Indeed, these three bands become more defined upon prolonged heating (data not shown).

The spectra recorded after annealing at temperatures higher than 400 °C change markedly. None of the bands present in Figs. 1a or b are present in Fig. 1c apart from the band at 723 cm^{-1} in Fig. 1b assigned to the O–W–O stretching vibration of monoclinic WO_3, which shifts to 715 cm^{-1} in the spectra of the films annealed at 500 °C. The terminal W = O stretching mode at 963 cm^{-1} is now absent, as are the modes assigned to O–W–O vibrations of amorphous WO_3, which are replaced by strong bands at 271 and 805 cm^{-1} assigned to the O–W–O bending and stretching modes of monoclinic WO_3, respectively [11]. Indeed, the bands present in Figs. 1c and d lie at almost exactly the same energies as those previously reported for monoclinic WO_3. There is no longer any evidence for the presence of carbon in the spectra, indicating the complete combustion of the organic additive. A significant increase in the signal-to-noise ratio is observed on increasing the annealing temperature from 500 to 550 °C. The spectra of the WO_3 films annealed at 550°C are at least twice as strong as those annealed at 500 °C, making the characteristic weak bands of monoclinic WO_3 at 435 and 447 cm^{-1} clearly visible. Such an increase in the strength of the spectrum is indicative of an increased crystallinity of the monoclinic phase.

In order to monitor the effect of the precursor material, thin films have also been prepared using tungsten (VI) ethoxide. The Raman spectrum of WO_3 film annealed at 500 °C (Fig. 2a) displays an intense band at 961 cm^{-1} along with overlapping bands at 648 and 685 cm^{-1}; a weak peak at 245 cm^{-1} is also observed. Interestingly, these bands closely correspond to those at 960, 685 and 662 cm^{-1} from $WO_3.2H_2O$ [11]. Evidence has been found of the presence of hydroxyl and H_2O species in the infrared spectrum of the film. Furthermore, even after annealing at 500 °C, clear evidence for the presence of carbonic species remains in the Raman spectrum. The spectrum of a film annealed at 300 °C, Fig. 2b, was difficult to interpret due to an increased

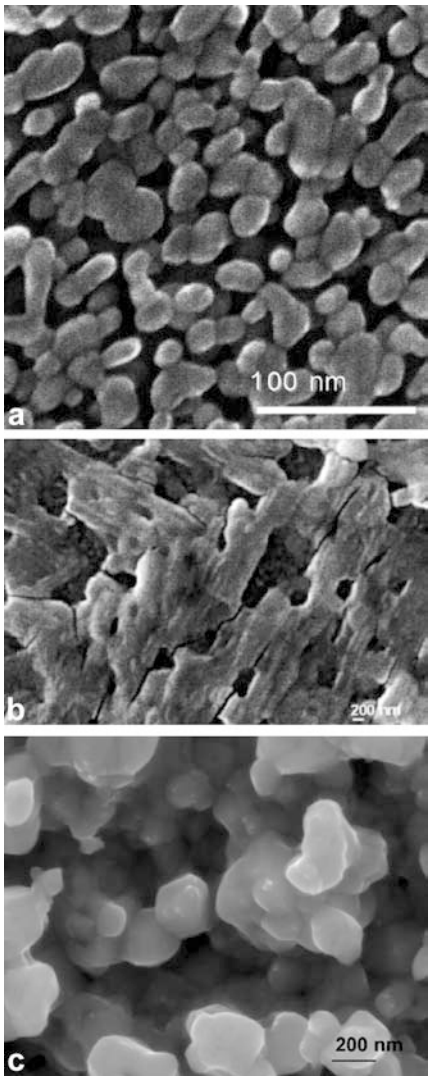

Fig. 4 Scanning electron micrograph images of WO_3 films. Films were formed from **a** tungstic acid precursor, annealed at 500 °C; **b** tungsten (VI) ethoxide precursor annealed at 500 °C; **c** tungsten (VI) ethoxide precursor annealed at 300 °C, followed by additional annealing at 550 °C

sloping baseline originating from a competing fluorescence process. Such fluorescence is likely to come either from partially pyrolysed PEG or ethoxide, evidenced by the large graphitic bands at 1390 and 1591 cm^{-1}. Nevertheless, it seems likely from the presence of the W = O stretching vibration at 964 cm^{-1} and the broad feature centred around 780 cm^{-1} that some amorphous WO_3 is present. Extended annealing of this film for four hours at 550 °C (Fig. 2c) clearly shows the removal of any carbonic species along with a complete change to the monoclinic WO_3 phase.

The structural changes associated with the injection of H^+ ions were investigated. Figure 3a shows the Raman spectrum of the WO_3 film prepared after annealing at 350 °C and insertion of H^+ ions. The bands present at 780 and 962 cm^{-1} in Fig. 1a are drastically reduced in intensity, and features increase in the 200–450 cm^{-1} region. These bands have already been observed to be present in the spectra of WO_3 films after Li^+ insertion, so vibrations involving H^+ or Li^+ seem unlikely. Following the suggested mechanism of ion insertion [13]:

$$xM^+ + xe^- + \text{a - } WO_{3-y} = \text{a - } M_xWO_{3-y}$$

Lee et al proposed that the bands around 300 and 450 cm^{-1} arise from vibrations of the W^{5+}–O and W^{5+} = O bonds, respectively. The dramatic reduction in intensity of the W^{6+} = O stretching mode at 962 cm^{-1} therefore supports these assignments.

It is interesting to note, in connection with the increased electrochromic efficiency of the films annealed at 500 °C (vide infra), that the Raman spectra of these monoclinic WO_3 films also change markedly upon colouration. The O–W–O stretching mode at 805 cm^{-1} shifts to 815 cm^{-1} upon colouration, whereas the band previously attributed to O–W–O stretching at 715 cm^{-1} disappears. Furthermore, a broad feature at ~960 cm^{-1} appears upon colouration in Fig. 3c and grows further in intensity in Fig. 3d. The exact reasons for this behaviour are not clear and the appearance of the band in the W^{6+} = O stretching region upon colouration in a film that is essentially monoclinic in its bleached state warrants further investigation, although it appears possible that the insertion of H^+ may induce a structural change to a hydrated form of WO_3. The presence of new bands at ~220 and 380 cm^{-1} attributable to $WO_3.H_2O$ may support this hypothesis [11]. The latter band in particular was assigned to a W–OH_2 stretching mode. It should be noted that the transmission spectra of the films, which are sensitive to reoxidisation of the coloured films, do not change during the course of the experiments, implying that the changes in the Raman spectra reported above arise solely from the reduced WO_3 films.

SEM

The morphology of WO_3 films prepared from a tungstic acid precursor and organic stabiliser have previously been shown to be dependent upon the temperature at which the film is annealed [8]. Figure 4a shows the typical image obtained for a WO_3 film produced from a tungstic acid/PEG precursor after annealing at 500 °C. A porous film is observed with 10–25 nm diameter spherical features. The morphology of a WO_3 film prepared from a tungsten(VI) ethoxide/PEG precursor after annealing 500 °C (Fig. 4b) is considerably different to that of the film prepared from tungstic acid. Not only is there a significant decrease in porosity, but the size of the surface features are an order of magnitude larger. Rectangular plate-like features of dimensions of around 300×1000 nm are observed. A lack of porosity has been previously observed in WO_3 films containing

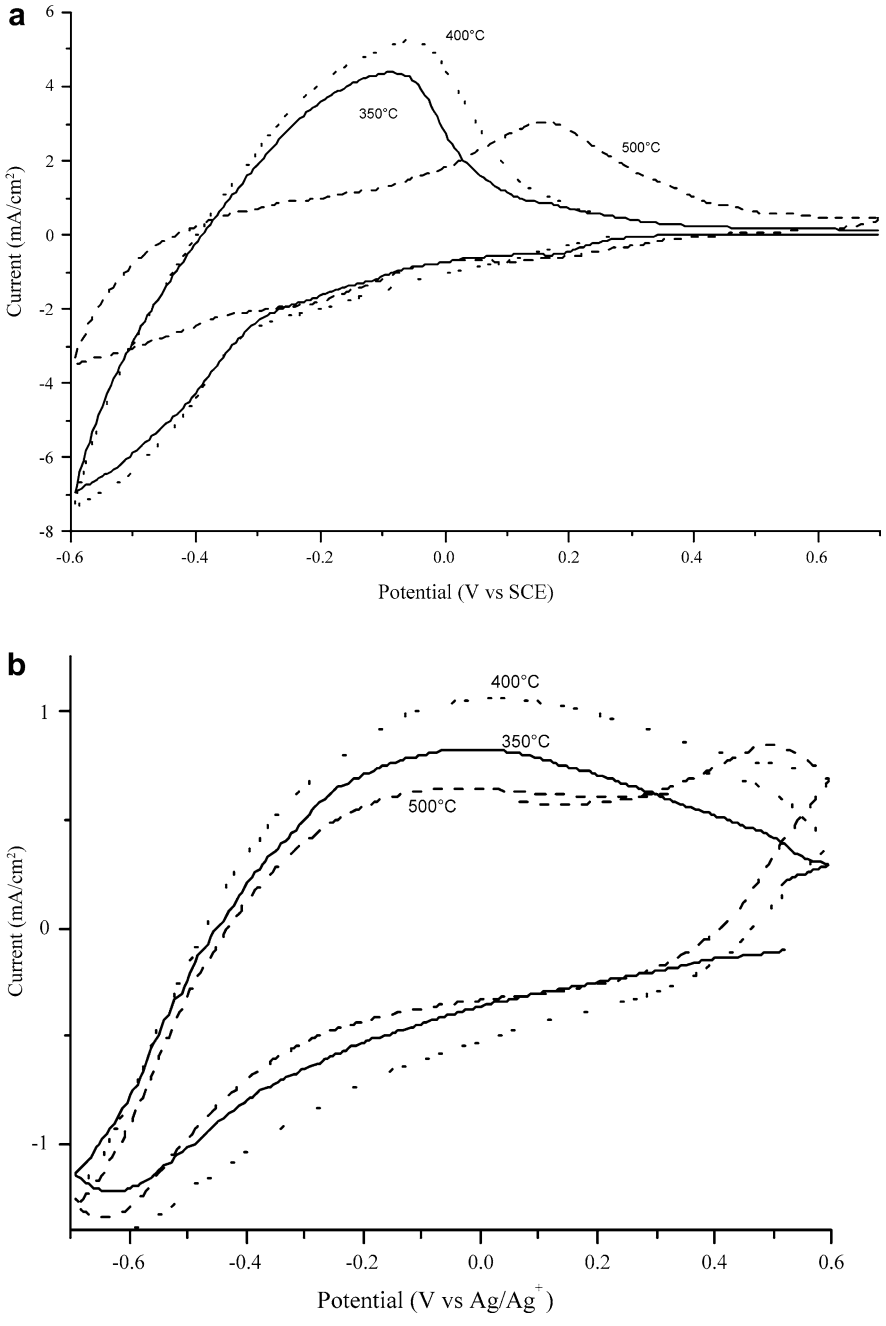

Fig. 5 Cyclic voltammograms of ~0.4 μm thick WO_3 films prepared from a tungstic acid/PEG precursor recorded at 50 mV/sec in **a** 1 M $H_2SO_{4(aq)}$ and **b** 1 M $LiClO_4$ in propylene carbonate

residual organic species, and this seems likely to be responsible for the effect shown in Fig. 4b. In such a case, it should be recalled that the same film was shown to consist of hydrated WO_3 and incompletely pyrolysed carbon (Fig. 2a). Increasing the temperature of annealing to 550 °C causes a substantial increase in porosity, shown in Fig. 4c, similar to the case of tungstic acid/PEG films. However, the spherical surface features of the monoclinic WO_3 films prepared from tungsten(VI) ethoxide remain substantially larger that those of the films derived from tungstic acid; the average particle size in Fig. 4c is around 200 nm.

Electrochromism

The electrochromic behaviour of the WO_3 films has been investigated in both an aqueous solution of H_2SO_4 (Fig. 5a) and $LiClO_4$ in propylene carbonate (Fig. 5b), and the transmittance spectra are shown in Fig. 6. For the film produced from tungstic acid after annealing at 500 °C (Fig. 6d) a high degree of transmittance (~90 %) is observed for wavelengths longer than 450 nm. Insertion of H^+ ions (Fig. 6c) produces a film which is no longer transparent to wavelengths above 600 nm. The transmittance of the WO_3 films prepared from tungsten

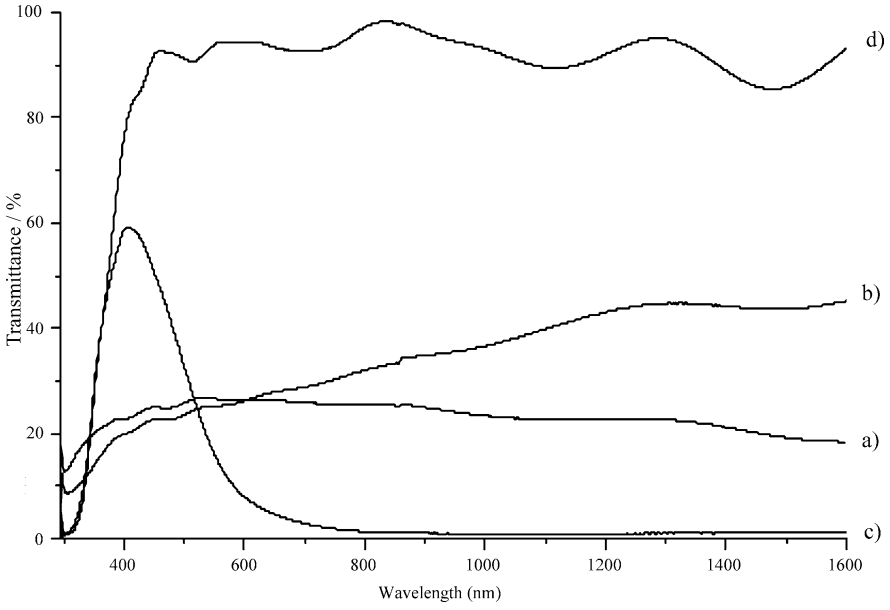

Fig. 6 Transmittance of WO_3 films annealed at 500 °C that were prepared from **a** tungstic hexaethoxide (coloured); **b** tungstic hexaethoxide (bleached); **c** tungstic acid (coloured); **d** tungstic acid (bleached)

hexaethoxide are considerably lower than those of prepared from tungstic acid (Figs. 6a and b). In fact, these films have been measured to be slightly thicker (by ~200 nm) than the films prepared from tungstic acid. Furthermore, the change in the transmittance spectrum upon colouration is typically small for films prepared using the tungsten hexaethoxide precursors: a fact probably linked to the lower porosity, as observed by SEM.

The change in optical density of the films relative to the amount of charge inserted – the colouration efficiency CE – is defined as:

$$CE = \frac{\Delta OD}{q}$$

where OD is the optical density and q is the charge inserted into the film. The CEs of the WO_3 films prepared from tungstic acid/PEG are shown in Fig. 7a for proton insertion and Fig. 7b for Li^+ insertion as a function of annealing temperature. For the insertion of protons, a maximum CE of 55 cm^2/C is obtained at 870 nm for films annealed at 500 °C. Films annealed at lower temperatures display maximum CEs of around 30 cm^2/C, typically at wavelengths longer than 1000 nm. The CEs for lithium insertion are clearly larger than those in Fig. 7a. In fact, the CE of 120 cm^2/C for the film annealed at 500 °C is much larger than previously reported values for WO_3 films. Djaoued et al [14] reported a CE of 66 cm^2/C for a film annealed at 300 °C, whereas we have previously reported that films annealed at 500 °C give CEs of 40 cm^2/C [8]. It should be noted that the film annealed at 300 °C reported herein shows a maximum CE of 87 cm^2/C, although at wavelengths shorter than the 1500 nm of Djaoued et al. Interestingly, the colouration efficiencies in Fig. 7b follow the trend 500 °C > 300 °C > 400 °C > 250 °C > 350 °C, and it seems that this ordering may result from two factors. The highest colouration efficiency is observed for films previously shown to be the most porous [14]. However, the question of crystal phase may also play an important factor in determining the values of the CEs. Amorphous WO_3 has been shown to be an excellent electrochromic material [15], and in line with the Raman data, which showed a substantially reduced intensity in films annealed at 400 °C, one might expect the decrease in amorphous WO_3 and subsequent increase in hexagonal WO_3 to be detrimental to colouration efficiency. The stability of the films has also been verified. No significant loss of performance was found for the WO_3 films prepared from the tungstic acid precursor when subjected to repetitive voltammetric cycling in $H_2SO_{4(aq)}$ for three days, indicating the good chemical and mechanical stability of the WO_3 films.

Photoelectrochemistry

As has already been noted [8, 9], WO_3 films have excellent photoelectrochemical properties. Although these are beyond the scope of this paper and are to be the subject of a future report [16], we will review the salient points. Photocurrents measured in 3 M H_2SO_4 under one sun irradiation show a clear dependence upon the annealing temperature. In fact, films annealed at temperatures less than 500 °C give photocurrents of 0.01 mA/cm^2 at most, whereas photocurrents from films annealed at 500 °C can attain values of 0.60 mA/cm^2. The spectral responses of the WO_3 films also show a similar dependency. Incident photon-to-current conversion efficiencies, IPCEs, display a clear maximum of 45 % at 300 nm for films annealed at 500 °C, whereas films annealed at lower temperatures are around 2%. This indicates that the presence of monoclinic WO_3 is indispensable for good photoelectrochemical behaviour.

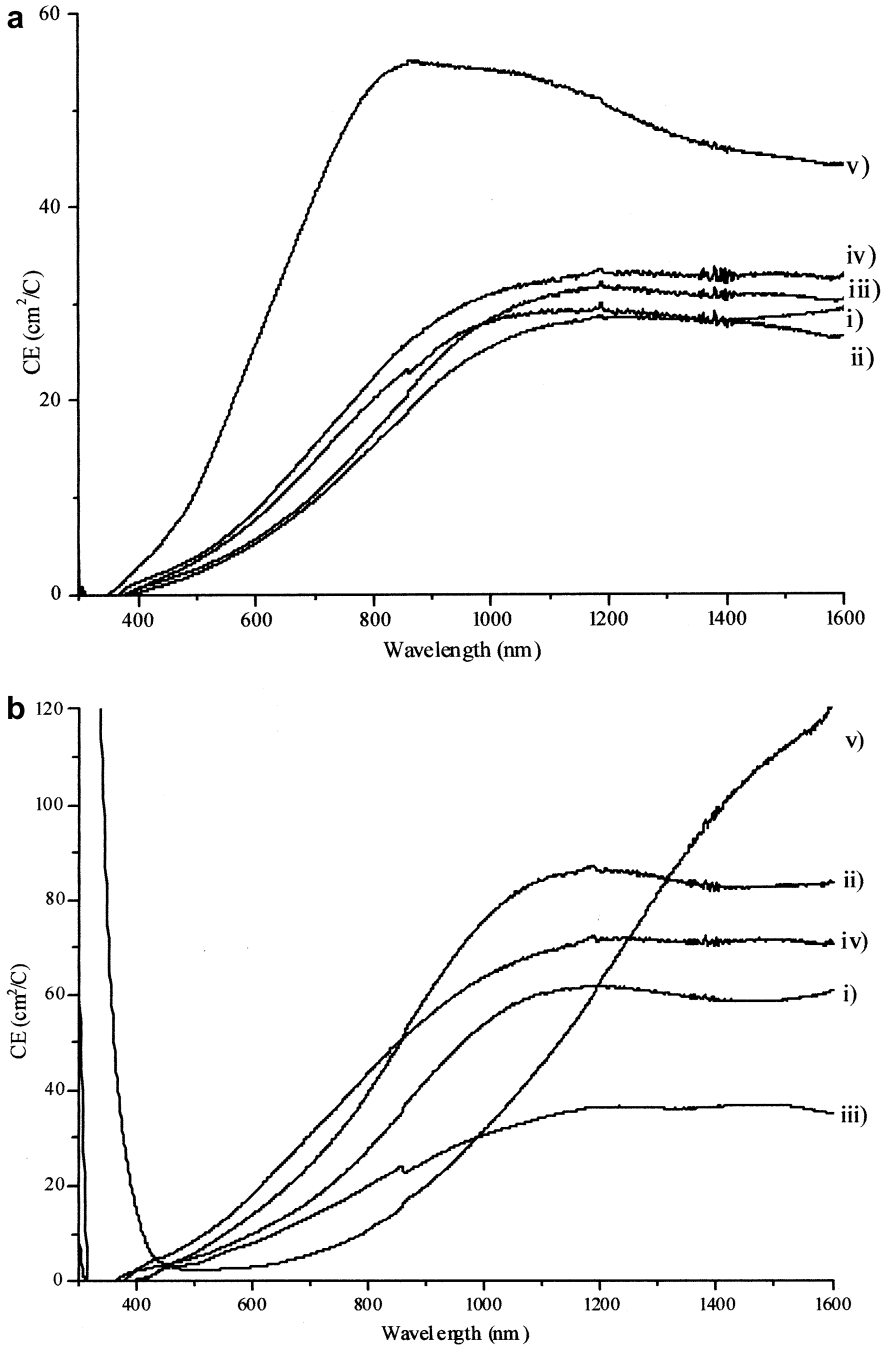

Fig. 7 Colouration efficiency (CE) of ~0.4 μm thick WO_3 films prepared from tungstic acid/PEG precursor in **a** 1 M $H_2SO_{4(aq)}$ and **b** 1 M $LiClO_4$ in propylene carbonate solutions. Films were annealed at **i** 250 °C; **ii** 300 °C; **iii** 350 °C; **iv** 400 °C; **v** 500 °C

Conclusions

Use of the sol-gel method, involving both a precursor of the oxide and an organic structure-directing agent, for the preparation of thin mesoporous WO_3 films imposes clear limits with regard to the conditions of heat treatment. The observed ordering of the film is closely related to the fact that the poly(ethylene glycol) employed in this work delays the crystallisation of WO_3, moving it to higher temperatures. In fact, formation of well-crystallised monoclinic WO_3 requires annealing at ~500 °C for the films fabricated using a tungstic acid precursor or even at 550 °C for those originating from tungsten ethoxide. These well-crystallised films combine good adherence and mechanical stability with the best electrochromic colouration efficiency. Interestingly, the same films also exhibit superior photoelectrochemical activity. These results might appear to be in contradiction with previously reported good electrochromic characteristics of amorphous WO_3 films. However, due to the thermal stability of PEG (and of its complexes with the precursors) both our amorphous and metastable hexagonal WO_3 films still contain substantial amounts of carbonaceous

species which seem to be detrimental to the electrochromic efficiency.

Acknowledgements This work was supported by the Swiss National Science Foundation and the Swiss Federal Office of Energy.

References

1. Kresge CT, Leonowicz ME, Roth WJ, Vartuli JC, Beck JS (1992) Nature 359:710
2. Inagaki S, Fukushima Y, Kuroda K (1993) J Chem Soc Chem Comm 8:680
3. Huo Q, Margolese DI, Ciesla U, Demuth DG, Feng P, Gier TE, Sieger P, Firouzi A, Chmelka BF, Schüth F, Stucky GD (1994) Chem Mater 6:1176
4. Antonelli DM, Ying JY (1995) Angew Chem Int Edit 34:2014
5. Tian Z, Tong W, Wang J, Duan N, Krishnan VV, Suib SL (1997) Science 276:926
6. Yang P, Zhao D, Margolese DI, Chmelka BF, Stucky GD (1998) Nature 396:152
7. Orton W, Powell MJ (1980) Rep Prog Phys 43:1263
8. Santato C, Odziemkowski M, Ulmann M, Augustynski J (2001) J Am Chem Soc 123:10639
9. Santato C, Ulmann M, Augustynski J (2001) J Phys Chem B 105:936
10. Nonaka K, Takase A, Miyakawa K (1993) J Mater Sci Lett 12:274
11. Daniel MF, Desbat B, Lassegues JC, Gerand B, Figlarz M (1987) J Solid State Chem 67:235
12. Lee S, Cheong HM, Tracy CE, Mascarenhas A, Benson DK, Deb SK (1999) Electrochim Acta 44:3111
13. Faughnan BW, Crandall RS, Heyman PM (1975) RCA Rev 36:177
14. Djaoued Y, Ashrit PV, Badilescu S, Brüning R (2003) J Sol-Gel Sci Techn 28:235
15. Lee S, Cheong HM, Zhang J, Mascarenhas A, Benson DK, Deb SK (1999) Appl Phys Lett 74:242
16. Solarska R, Alexander BD, Augustynski J (2004) unpublished results